RESEARCH CONCERNING MACHINING SOME ALLOYS OF Co, Cr AND Ti BY MILLING AND ELETRICAL DISCHARGE MACHINING

DINCĂ Cristian-Daniel[1], FRANCISC Petre[1] and GHICULESCU Liviu Daniel[2]
Faculty of Industrial Engineering and Robotics, Specialty: Manufacturing Engineering, Year of study: IV,
e-mail: cristi1999dinca@gmail.com
[2]Faculty of Industrial Engineering and Robotics, Manufacturing Engineering Department
University POLITEHNICA of Bucharest

ABSTRACT: The paper deals with the comparison of machining alloys based on Co, Cr and Ti, Al between mechanical processes, like milling and nonconventional thermal processes, like electrical discharge machining (EDM). The studied materials have great characteristics of resistance, corrosion, some like Co, Cr alloys are biocompatible, and some others like Ti, Al alloys have high resistance at big temperature. Generally, they are difficult to be cut, therefore EDM was used at cavity machining in comparison and combination with milling. Finally, a finite element modelling of EDM process was approached to better understand the thermal removal mechanism of these materials. Experimental data proved that CoCr alloys have higher machinability than Ti, Al alloys at both types of processes used.

KEYWORDS: alloys Co, Cr, Ti, milling, electrical discharge machining

1. Introduction

For this study it was necessary to purchase semifinished products made of CoCr alloys and Ti aluminide and to process them by milling and electrical discharge machining (EDM). It was first necessary to mill the semifinished products using a milling cutter with a diameter of Φ10 mm, in order to obtain flat surfaces. Using a cylindrical-front milling cutter with a diameter of 2 mm and, respectively, massive copper electrodes, cavities of 5x5x1,5 mm were made, and the quality of the surfaces obtained by the two processing processes was analyzed.

2. Current stage

Fields of application of Co, Cr and Ti alloys: Due to their excellent characteristics of corrosion resistance, wear resistance, high creep resistance, high temperature resistance and good biocompatibility, CoCr alloys have applications in many engineering fields such as turbomotors, nuclear, biomedical, and dentistry [1]. CoCr alloys are also widely used in other fields of medicine: stents [2], intervertebral disc replacement, knee or hip arthroplasty [3,4]. These alloys achieve their corrosion resistance by forming chromium-based oxides on the surface, and their biocompatibility then becomes extremely valuable over time [5].

High-pressure compressors use conventional titanium alloys (α and α-β) in areas where the working temperature does not exceed 500°C [6]. TiAl-based alloys are especially suitable for applications of low-pressure turbine blades and high-pressure compressor blades [7]. General Electric said that the low-pressure turbine blades in the TiAl range manufactured by Precision Castparts Corp. were used in GEnx engines, which equipped Boeing 787 / Boeing 747-8 aircraft [8].

Properties of Co, Cr and Ti alloys: The main hardening mechanism of cobalt-based alloys is the formation of carbides, solid solution hardening and the formation of intermetallic compounds, acting in the same direction. The carbides disperse in the alloy matrix and precipitate at the granule boundaries, and this dispersion has a direct effect on the mechanical strength of the alloy [9].

Titanium γ (TiAl) aluminum has the highest specific stiffness compared to all other classes of alloys. At the same time, titanium aluminum alloys have high values of modulus of elasticity, compared to conventional titanium alloys and nickel-based alloys [6].

Tables 1 and 2 show the chemical composition of some CoCr alloys and titanium aluminides, respectively.

Table 1. Chemical composition of CoCr alloys used in experiments [10,11]

Alloy	Cr [%]	Mo [%]	W [%]	Nb [%]	Si [%]	Mn [%]	Fe [%]	Co [%]
P1, SYSTEM NE	21,0	6,5	6,4	-	0,8	0,65	<0,1	64,4
P2, SYSTEM SOFT	29,5	5,7	-	-	0,95	0,55	0.75	61,8
P3, LUKA CHROM	24,0	3,0	8,0	1,0	1,0	-	-	63,0

Table 2. Chemical composition of titanium alumina used in experiments [12]

Alloy	Alloy element	Ti	Al	Nb	Cr	Zr	Ta	B	α_2 phase %
Alloy 1	at %	45	44	4	-	4	1	1	2
Alloy 2	at %	43	47	7	1	-	0.5	-	25

Tables 3 and 4 show the mechanical properties of some CoCr alloys and titanium aluminides, respectively.

Table 3. Mechanical properties of CoCr alloys used in experiments [10,11]

Alloy	Tensile strength [MPa]	Young Modulus [GPa]	Elastic limit [MPa]	Breaking elongation [%]	Hardness [HV]
P1, SYSTEM NE	850	155	580	3	460
P2, SYSTEM SOFT	447	160	450	15	310
P3, LUKA CHROM	550	125	545	25	185

Table 4. Mechanical properties of titanium aluminates [12]

Alloy	Tensile strength, at 25°C, [MPa]	Tensile strength, at 760°C, [MPa]	Breaking elongation, at 25°C, [%]
Alloy 1 (1, 2, 3 samples)	620	550	3
Alloy 2 (4, 5 samples)	1100	620	2-3

Alloys based on intermetallic compounds γ (TiAl) and α_2 (Ti_3Al) have important thermo-physical and mechanical properties, such as: high melting point, above 1460°C, low density (3,9-5 g/cm^3, depending on the degree alloy), high stiffness, yield strength and creep resistance at high temperatures, structural stability at high temperatures, low diffusion coefficient.

Alloys P1 and P3, which contain W, have a slightly higher thermal conductivity compared to alloy P2, as this alloying element has the highest heat transfer coefficient: 170 [$W*m^{-1}*K^{-1}$] [13] . According to the literature, the specific heat of CoCrMo ternary alloys (similar to alloy 2) is 452 $J*Kg^{-1}*K^{-1}$ [14].

3. Milling materials processing. Technological stages

Figures 1 and 2 show the samples of CoCr alloys according to the notation in Table 5, respectively titanium aluminide, which were subjected to milling processing according to the notation in Table 4.

Fig. 1 Samples of CoCr alloys

Fig. 2 Titanium aluminide samples

The stages of the technological milling process were:
1) Milling of semi-finished products using a milling cutter with a diameter of Φ10 mm, in order to obtain flat outer surfaces
2) 3D modeling of the part in the Autodesk Inventor 2023 design software

3) Carrying out the processing to obtain cavities of 5x5x1.5 mm (fig. 3, 4); a Φ2 mm milling cutter was used, the machining being performed on the numerically controlled machining center, Deckel Maho DMU70 (fig. 5) using the HEIDENHAIN iTNC530 CNC programming software (fig. 6). The processing regime for roughing operation for CoCr and titanium alloy parts, respectively, is shown in Table 5.

Table 5. Processing arrangements for parts of CoCr and titanium aluminide alloys

Part	Processing regime					
	v_c [m/min]	n [rot/min]	f_z [mm/dinte]	f [mm/min]	z	a_p [mm]
CoCr alloy parts	30	4774	0,008	153	4	0,3
Titanium aluminide alloy parts	25	3979	0,006	95	4	0,3

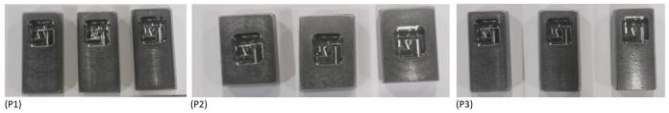

Fig. 3 CoCr alloy parts machined by milling

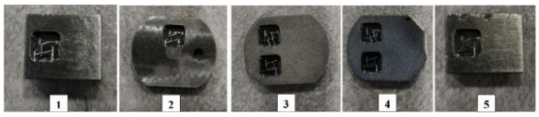

Fig. 4 TiAl alloy parts machined by milling


Fig. 5 CNC machining center, Deckel Maho DMU70


Fig. 6 HEIDENHAIN iTNC530 CNC Programs

4. Material processing by EDM. Technological stages.

1) Making copper electrodes (roughing electrode and finishing electrode), presented in fig. 7 was performed on the CNC machining center MAZAK NEXUS 350-II MY (fig. 8). The processing speed was 40 m/min for roughing turning, 50 m/min for finishing turning and 35 m/min for milling. Turning was performed with a roughing lathe knife (PWLNR 2525 M08 - WALTER) and a finishing lathe knife (SDHCR 2525 M11 - WALTER), and milling with a Φ6 mm milling cutter (MC111-06.0A4A-WJ30TF - WALTER).
2) The electrodes were checked and it was found that they fall within the tolerances included in the execution drawing (fig. 9). In order to determine the dimensions of the active part of the electrodes, respectively the size of the cross section (D_s) and the height (h_s), the relations were used [12]:

$$D_s = D_p - 2\,s_L \quad [mm] \quad (1)$$

$$h_s = h_p\,(1+\Theta) + c_s \quad [mm] \quad (2)$$

where: D_p - the size of the part cavity; s_L - side gap (from the ELER 01 car book); h_p - piece height [mm]; Θ - relative wear (from the ELER 01 car book) [%]; c_s - safety factor, c_s=3-5 mm.

The average roughness of the front surfaces is 0.230 μm and of the side surfaces is 0.325 μm when finishing milling.

Fig. 7 Roughing and finishing electrodes


Fig. 8 CNC Processing center MAZAK NEXUS 350-II MY

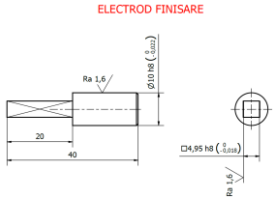

Fig. 9 Execution drawing of the finishing electrode

3) EDM was performed on the ELER 01 machine with the following regimes: roughing: controlled pulses, positive polarity at CoCr and negative at TiAl, I=6A (maximum current density was observed, J=I/S of 20 A/cm^2, S-front surface), impulse time, t_i=95 μs, pause time, t_0=24 μs; finishing: negative polarity, relaxation pulses, t_i≈0,8 μs, given by the capacity steps, C=10 nF and resistance, R=0,74 kΩ. In all regimes, the pulsating regime was adopted to facilitate the flushing of the working gap: 3s processing, 2s lifting;
The experimental data for roughing milling (FD) and roughing EDM (D) and finishing (F) are presented in Table 6.

Table 6. Experimental data on milling (FD) and roughing EDM (D) and finishing (F)

Material type	Processing Milling/EDM	Time [min]	t Milling/EDM [mm]	Volume Milling/EDM [mm^3]	Vw Milling/EDM [mm^3/min]	Ra Milling/EDM [μm]
P1, NE	FD/EDM D	1,03/6,67	1,2/1,45	30/36,25	29,13/5,43	0,473/1,285
P2, SOFT	FD/EDM D	1,03/9,80	1,2/1,45	30/36,25	29,13/3,70	0,435/1,233
P3, LUKA	FD/EDM D	1,03/7,12	1,2/1,45	30/36,25	29,13/5,09	0,447/1,214
P1 TiAl	FD/EDM D	1,46/12,90	1,2/0,10	30/2,5	20,55/0,19	0,513/1,451
P2 TiAl	FD/EDM D	1,46/8,58	1,2/0,15	30/3,75	20,55/0,44	0,422/1,376
P3 TiAl	FD/EDM D	1,46/11,50	1,2/0,15	30/3,75	20,55/0,33	0,407/1,522
P4 TiAl	FD/EDM D	1,46/10,53	1,2/0,18	30/4,5	20,55/0,43	0,403/1,395
P5 TiAl	FD/EDM D	1,46/7,74	1,2/0,18	30/4,5	20,55/0,58	0,438/1,408
P1, NE	EDM F	20,97	0,05	1,25	0,06	0,483
P2, SOFT	EDM F	25,52	0,05	1,25	0,05	0,435
P3, LUKA	EDM F	15,44	0,05	1,25	0,08	0,390
P1 TiAl	EDM F	36,44	0,05	1,25	0,03	0,801
P2 TiAl	EDM F	23,20	0,05	1,25	0,05	0,693
P3 TiAl	EDM F	17,05	0,05	1,25	0,07	0,898
P4 TiAl	EDM F	36,64	0,05	1,25	0,03	0,742
P5 TiAl	EDM F	13,17	0,05	1,25	0,09	0,773

According to the results obtained for roughing by EDM, it is found that in the case of titanium aluminide parts, the processing times even in the case of small processing depths are longer, compared to those recorded in the case of processing CoCr alloy parts.

Figures 9 and 10 show the cavities made by EDM and milling, respectively.

Fig. 9 Parts of CoCr alloys processed by EDM and milling

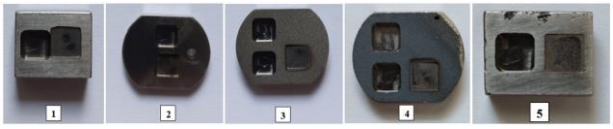

Fig. 10 Parts of TiAl alloys processed by EDM and milling

5. Control of piece

The roughness control of the cavity surfaces obtained by milling and EDM was performed with the Mahr MarSurf SD 26 roughness meter, the values obtained for roughness, being presented in table 6.

6. Finite element modeling of the EDM process

6.1 Model parameterization. Figures 11 and 12 show the parameters of the model in the Comsol Multiphysics 4.2 program for CoCr alloys, respectively, TiAl.

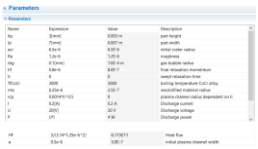

Fig. 11 Model parameters for CoCr alloys

Fig. 12 Model parameters for TiAl alloys

6.2 Creating the surface geometry after a single discharge: Fig. 13 shows the geometry of the surface geometry of a single discharge.

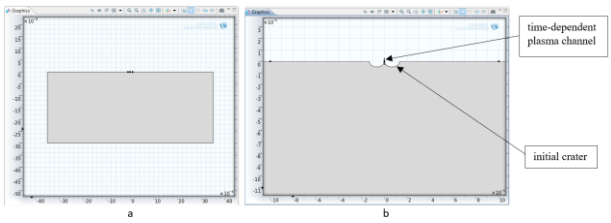

Fig. 13 Model geometry (a-part profile, b-microgeometry profile)

6.3 Introduction of material characteristics. Figures 14 and 15 show the material characteristics of the two types of materials.

Property	Name	Value	Unit	Property group
Density	rho	1000 [kg/m^...	kg/m^3	Basic
Thermal conductivity	k	9.4 [W/(m*K)]	W/(m*K)	Basic
Heat capacity at constant pressure	Cp	390 [J/(kg*K)]	J/(kg*K)	Basic

Fig. 14 Characteristics of CoCr alloys

Property	Name	Value	Unit	Property group
Heat capacity at constant pres...	Cp	520[J/(kg*K)]	J/(kg*K)	Basic
Density	rho	4000[kg/m^3]	kg/m^3	Basic
Thermal conductivity	k	55[W/(m*K)]	W/(m*K)	Basic

Fig. 15 Characteristics of TiAl alloys

6.4 Boundary conditions. Figures 16, 17, 18 show: heat flux, gas bubble insulation, dielectric cooling.

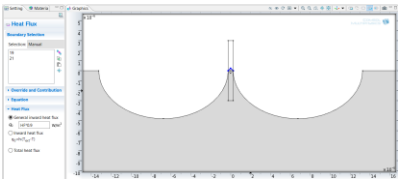

Fig. 16 Heat flux

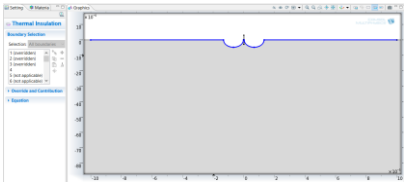

Fig. 17 Gas bubble insulation

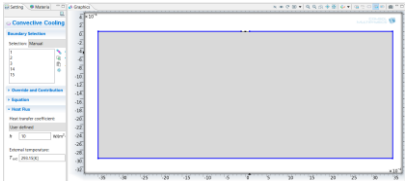

Fig. 18 Dielectric cooling

6.5 Results-temperature distribution after a single discharge on the two types of materials and discretization. Figures 19 and 20 show the temperature distributions after a single discharge on the two types of materials (in the case of CoCr alloys, the crater has a greater depth). Fig. 21 shows the discretization which has a dynamic character.

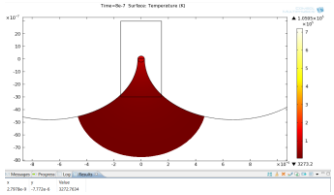

Fig. 19 Temperature distribution after a single discharge for CoCr alloys

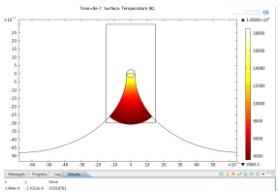

Fig. 20 Temperature distribution after a single discharge for TiAl alloys

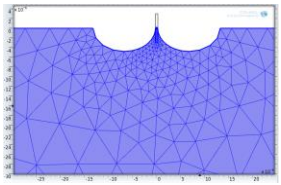

Fig. 21 Mesh

7. Conclusions

1. The experimental data obtained after processing the semi-finished products from the studied materials showed a higher machinability in both milling and EDM in the case of CoCr alloys, compared to Ti aluminides.

2. Analyzing the values obtained for the processing time and the productivity of each process used, it results that the variant that ensures a minimum time is the combination of roughing milling and finishing EDM necessary for the processing of the corners of the cavities.

3. Finite element modeling of the EDM process, respectively of a single discharge with relaxation impulse, used in finishing, shows that on the CoCr alloy a crater with a greater depth is obtained, compared to the depth obtained on the intermetallic compound, titanium aluminide, which results in the difference in productivity in the processing of the two materials.

8. Bibliography

[1]. Vaicelyte, A.; Janssen, C.; Le Borgne, M.; Grosgogeat, B. (2020), "Cobalt–Chromium Dental Alloys: Metal Exposures, Toxicological Risks, CMR Classification, and EU Regulatory Framework", *Crystals Vol. 10*, pag. 1151

[2]. Gherbesi, E. and Natalini, G. (2020). "The Ultimaster coronary stent system: 5-year worldwide experience", Future Cardiol., *Vol. 16*, pag. 251–261

[3]. Louwerens, J.K., Hockers, N., Achten, G., Sierevelt, I.N., Nolte, P.A., Van Hove, R.P. (2020). "No clinical difference between TiN-coated versus uncoated cementless CoCrMo mobile-bearing total knee arthroplasty; 10-year follow-up of a randomized controlled trial", *Knee Surg. Sports Traumatol. Arthrosc.*, pag. 1–7

[4]. Liu, G., Wang, X., Zhou, X., Zhang, L., Mi, J., Shan, Z., Huang, B., Chen, Z., Chen, Z. (2020). "Modulating the cobalt dose range to manipulate multisystem cooperation in bone environment: A strategy to resolve the controversies about cobalt use for orthopedic applications", *Theranostics Vol. 10*, pag. 1074–1089

[5]. Buser, D., Sennerby, L., De Bruyn, H. (2017)."Modern implant dentistry based on osseointegration: 50 years of progress, current trends and open questions", *Periodontology 2000 Vol. 73*, pag. 7–21.

[6]. Leyens, C. and Peters, M. (2003). "Titanium and titanium alloys: fundamentals and applications", Editura on line Wiley-VCH , 532 pag., 978-3-527-60211-7

[7]. Liu, B. and Liu, Y. (2015). "Powder metallurgy titanium aluminide alloys"-Capitol 27 în cartea "Titanium Powder Metallurgy", ISBN 978-0-12-800054-0, Copyright © 2015 Elsevier Inc. All rights reserved, 628 pagini

[8]. GE – Aviation: GEnx, GE [Online]. http://www.geae.com/engines/commercial/genx/, 2007

[9]. Mori, M. et al. (2012). "Microstructures and mechanical properties of biomedical Co-29Cr-6Mo-0.14N alloys processed by hot rolling", *Metallurgical and Materials Transactions*, Vol. *A 43(9)*, pag. 3108-3119

[10] https://adentatec.com/

[11] https://www.lukadent.de/

[12] Szkliniarz, W. and Szkliniarz, A. (2021) "Microstructure and Properties of TiAl-Based Alloys Melted in Graphite Crucible", *Metals, Vol. 11*, no. 4, pag. 669-686

[13]. https://periodictable.com/Properties/A/ThermalConductivity.an.htm

[14]. Baron, S., Ahearne, E., Connolly, P., Keaveney, S., Byrne, G. (2015). "An Assessment of Medical Grade Cobalt Chromium Alloy ASTM F1537 as a "Difficult-to-Cut (DTC)" Material", Proceedings of the Machine Tool Technologies Research Foundation Annual Meeting, San Francisco, June 30th-July 2nd, 2015

[15]. Ghiculescu, D. Curs de tehnologii Neconvenționale, available at https://curs.upb.ro/2021/login/index.php, Accessed at: 1.05.2022